

RECENT UNDERSTANDING AND IMPROVEMENTS OF THE LCLS INJECTOR*

F. Zhou,[†] D. Bohler, Y. Ding, S. Gilevich, Z. Huang, H. Loos, and D. Ratner
SLAC, Stanford, CA 94309, USA

Abstract

Ultraviolet drive laser and copper photocathode are the key systems for reliably delivering $<0.4 \mu\text{m}$ of emittance and high brightness free electron laser (FEL) at the linac coherent light source (LCLS). Characterizing, optimizing and controlling laser distributions in both spatial and temporal directions are important for ultra-low emittance generation. Spatial truncated Gaussian laser profile has been demonstrated to produce better emittance than a spatial uniform beam. Sensitivity of the spatial laser distribution for the emittance is measured and analysed. Stacking two 2-ps Gaussian laser beams significantly improves emittance and eventually FEL performance at the LCLS in comparison to a single 2-ps Gaussian laser pulse. In addition, recent observations at the LCLS show that the micro-bunching effect depends strongly on the cathode spot locations. The dependence of the micro-bunching and FEL performance on the cathode spot location is mapped and discussed.

INTRODUCTION

The cost and performance of the x-ray free electron laser (FEL) [1-2] depends critically on the emittance of the electron beam from the injector source. Producing and maintaining the desired ultra-small emittance ($<0.4 \mu\text{m}$ for 180-250 pC) is one of the major challenges for operations of Linac Coherent Light Source (LCLS). Major injector source emittance includes cathode thermal emittance, space charge, and RF-contributed emittance [3-4]. According to the LCLS operational experience, the photocathode drive laser distributions sensitively affect injector emittance thereby hard x-ray FEL performance. The LCLS drive laser system is a frequency tripled, chirped-pulse amplification system based on Ti:sapphire. The system consists of mode-locked oscillator, followed by a pulse stretcher oscillator, a regenerative amplifier, two multi-pass amplifiers, pulse compressor, and finally a frequency tripler to convert the IR laser to 253 nm. The 253 nm laser beam is finally delivered to the copper photocathode through a long in-vacuum transport from the laser room on the ground to the 10-m deep SLAC linac tunnel.

The performance of the complex LCLS laser systems is sensitive to the external environment such as humidity, temperature and dusts and aging equipment. For 24/7 operating laser systems, minor environment change may cause optical misalignments, even optics damage, resulting in changes of spatial and temporal laser

distributions on the cathode. Measuring, optimizing and controlling the desired spatial and temporal laser profiles on the cathode are of particular importance for maintaining the desired ultra-low emittance and maximizing x-ray FEL performance. As the drive laser systems, the LCLS copper photocathode is also of importance for the emittance and the micro-bunch instability (μBI). Recently we observed at the LCLS that the μBI is different at different cathode spots, causing different hard x-ray FEL performance (e.g., pulse intensity and bandwidth). Impacts of drive laser distributions and photocathode on the emittance, μBI and FEL performance are measured and analysed. This paper is organized as follows. Section II will introduce the measures of the spatial laser distribution and laser impacts on emittance. Emittance dependence on the temporal laser distribution is presented in Section III. In section IV, the dependence of the μBI and x-ray FEL performances on the laser location across the photocathode is mapped and discussed. The results are finally summarized.

MEASURING, OPTIMIZING AND CONTROLLING SPATIAL LASER DISTRIBUTION FOR ULTRA-LOW EMITTANCE

Many previous studies showed the drive laser must be uniform in transverse dimensions on the photocathode to produce the best emittance beam. However, recently simulations and experimental observations at the LCLS [5] show that the truncated-Gaussian spatial laser beam produces a better emittance beam than uniform laser does. Figure 1 (top) shows the different spatial lineout-intensity distributions including uniform-like (a), truncated-Gaussian (b), and Gaussian-like (c). The projected and time-sliced emittances of three distributions are simulated, as shown in Fig. 1 (bottom), using ImpactT code [6] for 150 pC. The emittance with the truncated-Gaussian distribution improves $\sim 30\%$ in comparison to the uniform-like laser or Gaussian-like beam.

Maintaining and controlling the spatial truncated-Gaussian laser beam on the photocathode, however, is not trivial for 24/7 operational laser systems. For example, it is difficult to maintain both shoulders a1 and a2 shown in Fig. 1(b) of the truncated-Gaussian distribution to be balanced through the complex laser systems and 10^3 meters-long laser transport. Extensive simulations show that the unbalanced shoulders increase the emittance. Therefore, having quantitative measures is crucial for characterizing, optimizing and controlling the spatial laser beam shapes and degree of asymmetry of both shoulders for ultra-small emittance beam. The following sub-

* The work is supported by DOE under grant No. DE-AC02-76SF00515.

[†] zhoufeng@slac.stanford.edu

sections describe two major measures (parameters for spatial laser lineout distribution and laser Zernike polynomials [7]) of the spatial laser shapes and emittance dependence on shapes. When the laser on the photocathode has regular smooth spatial distribution, either of two measures is good for quantitative characterization of laser beam. However, in reality, the laser distribution sometimes is irregular from the laser systems due to misalignment and mirror damages. In such a case, using parameters for lineout laser distribution may not fully represent a true laser beam, as only emittance number cannot represent an irregular electron beam. The parameters for laser Zernike polynomials are found as a better measure of the laser spatial distributions for the case, although it is more complicated. With these two vital measures, the desired parameters for spatial laser distribution can be maintained within the criteria for high-brightness electron beam generation.

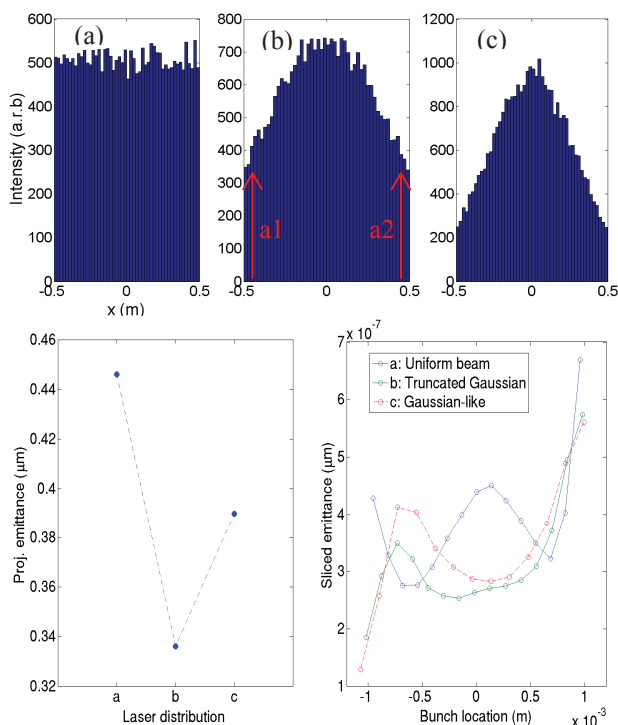


Figure 1: Spatial laser lineout distributions (top), (a), (b) and (c) represent uniform-like, certain truncated-Gaussian and Gaussian-like spatial distributions; corresponding projected (bottom, left) and slice emittances (bottom, right) for 150 pC.

Parameterized With Lineout Laser Distribution

When the laser spatial distribution is reasonably smooth, as shown in Fig. 2, the method of using lineout-distribution is the best way to quantify laser profile. The lineout intensity ratio g/h shown in Fig.2 is used to determine the laser shape. The laser is in uniform-like with $g/h < 0.1$, while it is close to Gaussian distribution with $g/h > 3$. Figure 3 shows both simulated (left) and measured (right) emittance for different laser lineout intensity ratio of g/h for 150 pC. Both measurements and

simulations show that the range of g/h for maintaining ultra-low emittance is in between 0.5 and 1.5. For a regular smooth-like spatial Gaussian laser beam, the lineout intensity ratio g/h can be adjusted within the desired range using an optical telescope.

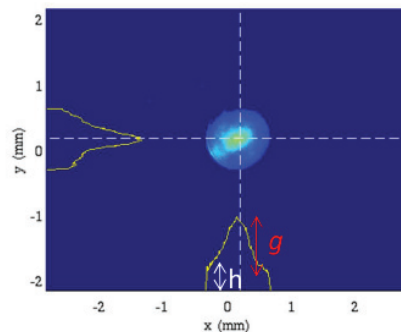


Figure 2: Example of regular smooth beam distribution parameterized by g/h of the lineout intensity ratio.

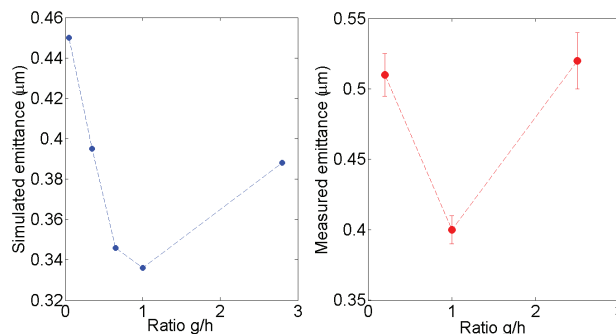


Figure 3: Simulated (left) and measured (right) emittance for different g/h of lineout intensity ratio for 150 pC.

Parameterized With Laser Zernike Polynomials

Zernike functions are usually used in the optical systems to characterize the measured structures of deformations and aberrations because these form a complete, orthogonal basis over the unit circle. The Zernike functions are a product of the Zernike radial polynomials and sine- and cosine-functions. As these functions are orthogonal on the unit circle, any function defined on the unit circle can be expressed as a sum of Zernike polynomials. The coefficients associated with the dominated Zernike polynomials can be used to represent optical data. For simplification, instead of using large amount of Zernike polynomials, two parameters [8], symmetry and asymmetry powers, are used to represent summed different types of polynomials for an optical spatial laser beam on the cathode. The symmetry power summing all symmetrical polynomials is to determine the spatial laser shapes, e.g., uniform or truncated Gaussian or Gaussian. In this study, the laser is close to uniform-like distribution with the symmetry power < 0.01 , while it is near Gaussian-like with the symmetry power > 0.07 . The asymmetry power summing asymmetrical polynomials is to determine the degree of laser beam symmetry with respect to the centroid spot location. The

laser beam is near symmetry with the asymmetry power <0.01 , otherwise the beam is in not symmetric. For a fixed asymmetry power <0.01 , emittance dependence on the symmetry power for different spatial laser shapes shown in Fig. 4 (top, a, b and c) is measured, as shown in Fig. 4 (bottom), for 150 pC. The data shows that the small emittance can be achieved with the symmetry power in 0.025-0.04 (truncated Gaussian distributions). Figure 5 shows the measured emittance dependence on the laser beam asymmetry power for a fixed symmetry power of 0.025. It shows the beam emittance can be maintained at ultra-low value with the asymmetry power <0.015 .

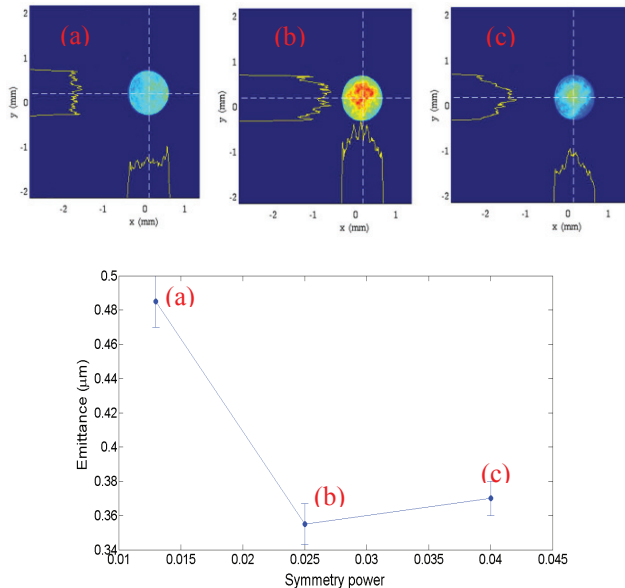


Figure 4: Laser shapes and related symmetry power vs. measured emittance for a fixed asymmetry power <0.01 .

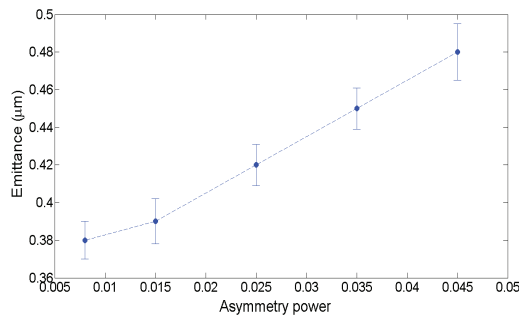


Figure 5: Measured emittance dependence on the asymmetry power for a fixed symmetry power of 0.025.

OPTIMIZATIONS OF TEMPORAL LASER DISTRIBUTION FOR ULTRA-LOW EMTTANCE

RF and space charge emittance strongly depends on the photocathode drive laser pulse length [9], expressed by:

$$\varepsilon_{rf} \sim E \cdot \sigma_r^2 \cdot \sigma_z^2 \quad (1)$$

$$\varepsilon_{sc} \sim \frac{Q}{E \cdot \sigma_z} \mu_x \quad (2)$$

where E is the peak accelerating gradient on cathode, μ_x is the transverse space charge factors related to the aspect ratio of the rms beam size σ_r to rms bunch length σ_z , and Q is the bunch charge. Eqs. 1 and 2 indicate that the laser pulse length has to be traded off for space charge and RF emittance for optimum emittance. Systematic simulations of the emittance dependence on the single Gaussian laser are performed for 180 pC, as shown in Fig. 6. The projected (left) and sliced emittance (right) is close to optimum for single ~ 3.5 ps FWHM Gaussian laser.

Current LCLS drive laser pulse has 1.9 ± 0.2 ps FWHM, and the laser systems are not flexible to lengthen laser pulse length >3 ps FWHM without compromising the laser temporal profile. Recently, two ~ 1.9 -ps different polarization Gaussian lasers are stacked together to lengthen the laser pulse. The advantages using pulse stacking over single Gaussian laser: 1) easier to adjust overall laser pulse length for various needs; 2) relatively sharper edges of the final laser pulse for emittance compensation process. As shown in Fig. 6, a better projected emittance is simulated with a stacked 4 ps pulse (~ 2 ps separation for stacking two 2-ps pulses) than single 3.5 ps Gaussian laser, although the slice emittance with 4 ps stacked laser is similar to 3.5 ps single Gaussian. The 4 ps stacked pulse has better emittance compensation than single 3.5ps Gaussian.

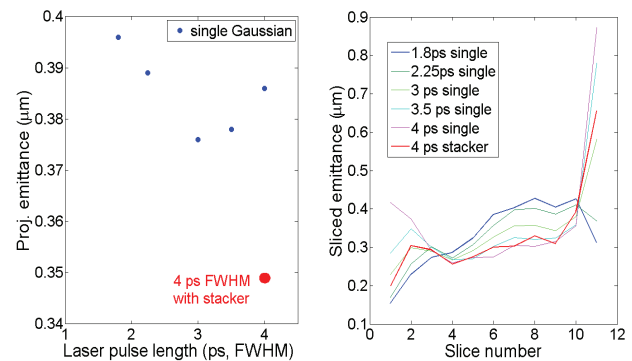


Figure 6: Simulated projected (left) and slice (right) emittance dependence on the single Gaussian laser and a stacked pulse 4 ps FWHM for 180 pC.

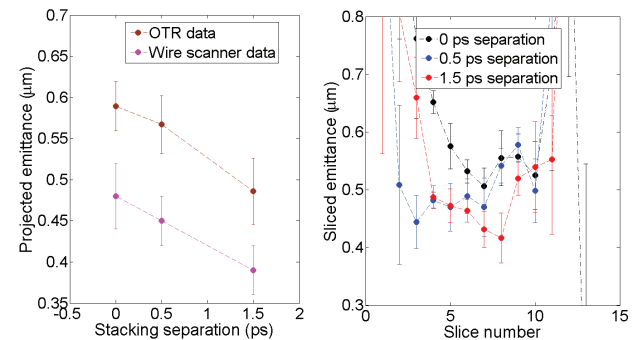


Figure 7: Measured projected (left) and slice (right) emittance (250 pC) with different separation for stacking two ~ 1.9 ps FWHM pulses.

Figure 7 shows the comparison of the measured projected (left) and slice (right) emittance for single Gaussian and stacked laser beam. At the LCLS, projected emittance can be measured with one OTR screen and wire scanner. The data shows the projected emittance measured with the OTR screen is ~20% higher than wire scanner. The higher emittance with the OTR method is probably caused by the microbunching effect at the OTR screen. Further understanding for the emittance difference using OTR and wire scanner is needed. The slice emittance can be measured only with the OTR screen and a transverse RF cavity. Although the measured projected and slice emittance using the OTR screen may be overestimated in comparison to wire scanner, the measured trend clearly shows emittance with stacked pulse is significantly improved compared with a single Gaussian laser for 250 pC. During the emittance measurements the spatial laser profile on the cathode is not setup for optimum emittance but it is kept unchanged for fair comparisons. The stacked laser pulse eventually improves the x-ray FEL pulse intensity by 30-50% compared with single Gaussian ~2 ps FWHM laser pulse.

MAPPING MICRO-BUNCHING OF THE PHOTOCATHODE

Micro-bunching as well as emittance plays critical roles on the x-ray FEL performance. Laser heater [10] in principle can suppress the μ BI, but cannot completely eliminate its effect thereby resulting in deterioration of FEL qualities such as pulse intensity and/or bandwidth. Photocathode is one of the major sources inducing the μ BI. Recently the micro-bunching effects observed at the LCLS cathode are found very different for different spots on the same cathode. We measured the coherent optical transition radiation (COTR) effect (i.e., integrated counts) at one OTR screen located immediately after the 1st stage of magnetic bunch compressor (BC1). 1-mm-size of laser spot is used to scan across the cathode with 0.1 mm of step size. The COTR signal on the cathode is mapped, as shown in Fig. 8.

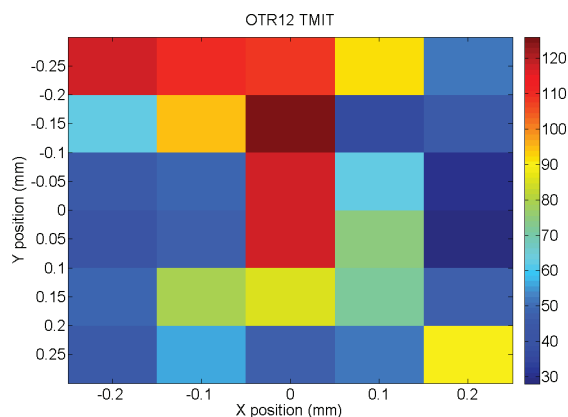


Figure 8: Measured COTR signal in arbitrary units for different laser locations on the same cathode.

The micro-bunching effect on different spots on the same cathode can vary by a factor of 3-4. The effect is expected to be significantly magnified through next magnetic bunch compressor and long-distance beam transport. A question is naturally asked: how is the different spot location correlated to different μ BI?

Subsequent measured electron emission profiles are found different for different spots on the cathode, and also the measured QE uniformity varies with the spot location. The resulting different uneven electron emission profile is probably caused by the recent laser cleaning [11-12] for the increase of QE for the copper photocathode. The different transverse electron emission profiles on the photocathode may induce different transverse space charge forces on the beam. A recently developed analytical model [13] may qualitatively explain how to transform the transverse into the longitudinal effects. In the model, for a finite angular spread x_0' with an initial uniform longitudinal coordinate but have a relative energy modulation of δ , when the beam enters dispersive area, transverse and longitudinal coordinates x and z are correlated, expressed by:

$$x = R_{12}x_0' + R_{16}\delta \cos[k(z - R_{52}x_0')] \quad (3)$$

where R_{12} , R_{52} , and R_{16} are transfer matrix, k is the oscillation wave number for energy modulation. With this correlation, transverse space charge induced by microstructure (such as uneven surface on the cathode) may couple to longitudinal plane to generate permanent longitudinal microbunching via leaked-out dispersions.

The measurements indicate that the FEL pulse intensity and/or bandwidth are correlated to different laser spot locations, as given in Table 1. As discussed above, different spot location is correlated to different micro-bunching on the cathode. The microbunching caused extra energy spread resulting in lower FEL pulse intensity or larger bandwidth. The data presented in Table 1 may indicate lower FEL pulse intensity or wider bandwidth is probably correlated to worse microbunching effects. Further thorough understanding for the observations is needed.

Table 1: Measured FEL performance and micro-bunching effect for different locations on the cathode. (Note N/A means the data is not measured).

Laser position x/y in mm	FEL pulse intensity	FEL bandwidth, FWHM	COTR signal (a.r.b.)
+0.2/-0.3	2.1 mJ	N/A	50
+0.2/+0.2	0.8-1 mJ	N/A	90
+0.2/-0.25	N/A	27 eV	50
-0.1/-0.25	N/A	40 eV	110

SUMMARY

Controlling spatial laser distribution on the cathode is of importance for ultra-low emittance beam. Quantitative measures of laser spatial distribution using parameters for lineout intensity and Zernike polynomials are developed. According to simulation and measurement results, optimum emittance are achieved and maintained with truncated-Gaussian spatial laser distribution, g/h in between 0.5-1.5 using lineout distribution measure or symmetry power in between 0.025-0.04 using Zernike polynomials measure. Simulations and measurements also concluded ultra-small emittance is achieved with 3.5-4 ps either single Gaussian or stacked laser pulse for 180-250 pC. Following these quantified criteria for spatial and temporal laser profiles, ultra-low emittance beam can be maintained.

The micro-bunching effects are found different for different cathode spots. The observations indicate that the FEL pulse intensity or bandwidth could be correlated to the micro-bunching effect for different spots. It is believed that different electron emission profiles at different cathode spot location causes different transverse space charge, which is eventually transformed into longitudinal space charge via the leaked dispersion along the beam transport. The longitudinal microbunching effect affects the energy spread thereby x-ray FEL performance.

REFERENCES

- [1] P. Emma et al., "First lasing and operation of an Angstrom-wavelength free electron laser", *Nature Photon.* 4 641 (2010).
- [2] T. Ishikawa et al., "A compact x-ray free electron laser emitting in the sub-angstrom region", *Nature Photonics* 6, 540-544 (2012).
- [3] K.-J. Kim, *Nucl. Instrum. Methods Phys. Res. Sect. A* 275, 201 (1989).
- [4] F. Zhou et al., "Experimental characterization of emittance growth induced by the nonuniform transverse laser distribution in a photoinjector", *Phys. Rev. ST-AB* 5, 094203 (2002).
- [5] F. Zhou et al., "Impact of the spatial laser distribution on photocathode gun operation", *Phys. Rev. ST-AB* 15, 090701 (2012).
- [6] J. Qiang, *ImpactT code manual*, LBNL-62326, 2007.
- [7] Zernike function see link below:
https://en.wikipedia.org/wiki/Zernike_polynomials
- [8] D. Bohler, private communication.
- [9] K.-J. Kim, "RF and space charge effects in laser-driven RF electron guns", *Nucl. Instrum. Methods*, A275, 201 (1989).
- [10] Z. Huang *et al.*, "Measurements of the linac coherent light source laser heater and its impact on the x-ray free-electron laser performance", *Phys. Rev. ST Accel. Beams* 13, 020703 (2010).
- [11] F. Zhou et al., "High-brightness electron beam evolution following laser-based cleaning of a photocathode", *phys. Rev. ST-AB* 15, 090703 (2012).
- [12] F. Zhou et al., "Establishing reliable good initial quantum efficiency and in-situ laser cleaning for the copper cathodes in the RF gun", *Nucl. Instru. Methods in Phys. Res. Section A* 783 (2015).
- [13] M. Venturini and J. Qiang, "Transverse space charge induced microbunching instability in high-brightness electron bunches", *Phys. Rev. ST-AB* 18, 054401 (2015).